

# Thermodynamics of Quantum Phase Transitions of a Dirac oscillator in a homogenous magnetic field

A. M. FRASSINO,<sup>1</sup> D. MARINELLI,<sup>2</sup> O. PANELLA,<sup>3</sup> and P. ROY<sup>4</sup>

<sup>1</sup>Frankfurt Institute for Advanced Studies, Ruth-Moufang-Straße 1, D-60438 Frankfurt am Main, Germany

<sup>2</sup>Machine Learning and Optimization Lab., RIST, 400487 Cluj-Napoca, Romania\*

<sup>3</sup>Istituto Nazionale di Fisica Nucleare, Sezione di Perugia, Via A. Pascoli, I-06123 Perugia, Italy†

<sup>4</sup>Physics and Applied Mathematics Unit, Indian Statistical Institute, Kolkata-700108, India

(Dated: July 24, 2017)

The Dirac oscillator in a homogenous magnetic field exhibits a chirality phase transition at a particular (critical) value of the magnetic field. Recently, this system has also been shown to be exactly solvable in the context of noncommutative quantum mechanics featuring the interesting phenomenon of re-entrant phase transitions. In this work we provide a detailed study of the thermodynamics of such quantum phase transitions (both in the standard and in the noncommutative case) within the Maxwell-Boltzmann statistics pointing out that the magnetization has discontinuities at critical values of the magnetic field even at finite temperatures.

## I. INTRODUCTION

Quantum Phase Transitions (QPT) [1] are a class of phase transitions that can take place at zero temperature when the quantum fluctuations, required by the Heisenberg's uncertainty principle, cause an abrupt change in the phase of the system. The QPTs occur at a critical value of some parameters of the system such as pressure or magnetic field. In a QPT, the change is driven by the modification of particular couplings that characterise the interactions between the microscopic elements of the system and the dynamics of its phase near the quantum critical point.

For a quantum system at finite temperature  $T$ , both the thermal and the quantum fluctuations are present. The interplay between the quantum and the thermal fluctuations can either smooth out the differences between the phases (namely, no phase transition occurs at finite temperature) or there can be regimes in which some discontinuities hold, and a phase transition appears. Eventually, the thermal fluctuations prevail [1].

In this paper, we focus on a particular quantum system, namely the Dirac oscillator, at finite temperature  $T$  and with an additional constant magnetic field  $\mathbf{B}$ . The Dirac oscillator system including an interaction in the form of a homogeneous magnetic field is an exactly solvable system [2–6] and shows interesting properties. In particular, at zero temperature, if the magnitude of the magnetic field either exceeds or is less than a critical value  $B_{\text{cr}}$  (which depends on the oscillator strength), this combined system shows a *chirality phase transition* [7, 8]. Because of the phase transition, the energy spectrum is different for  $B > B_{\text{cr}}$  and  $B < B_{\text{cr}}$  where  $B$  is the magnetic field strength.

The  $(2 + 1)$ -dimensional Dirac oscillator in the presence of a constant magnetic field has also been studied at zero temperature in the framework of noncommutative

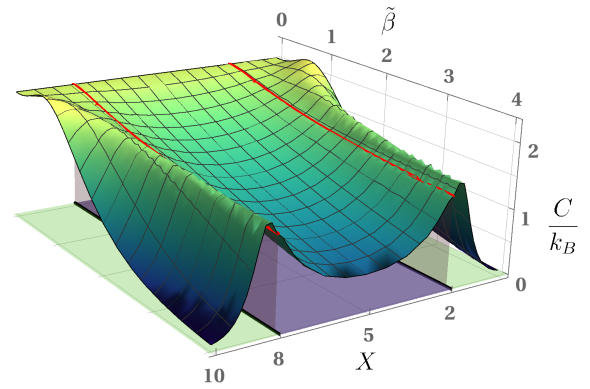


FIG. 1. Re-entrant phase transition as shown by the heat capacity of a noncommutative Dirac Oscillator as a function of the scaled effective magnetic energy  $X \equiv (\mu B - \hbar\omega)/mc^2$  and the scaled inverse temperature  $\tilde{\beta} = mc^2/k_B T$ .  $X_1 = \omega_\eta \hbar/mc^2 = 2$ ,  $X_2 = (\omega_\theta \hbar/mc^2) = 8$  are the two critical points that divide the green regions (left phases) from the violet region (right phase). In the left phases, the heat capacity is non-monotonic in  $\tilde{\beta}$ .

space coordinates and momenta [9]. It has been shown that in this case  $B_{\text{cr}}$  depends not only on the oscillator strength but also on the noncommutative parameters. An interesting consequence of the noncommutative scenario is that, apart from the left- and right-chiral phases of the commutative case [4], there is also a third left phase and thus a second quantum phase transition (right-left) [9] (see Fig. 1). The presence of the third phase with left chirality leads to what is called a Re-entrant Phase Transition (RPT) [10] first observed in nicotine/water mixture [11] as noted in [12]. This phenomenon has been recently found also in gravitational systems [13, 14].

In this work, we analyze the Dirac oscillator in the presence of a constant magnetic field at finite temperature. While in the first part of the paper we consider the standard system at finite  $T$ , the second part will be dedicated to the noncommutative Dirac oscillator.

\* Email: [marinelli@rist.ro](mailto:marinelli@rist.ro)

† Email: [orlando.panella@pg.infn.it](mailto:orlando.panella@pg.infn.it)

To study what kind of QPT the Dirac oscillator at finite  $T$  undergoes, we will investigate the system at high temperatures when the statistics can be approximated with the Maxwell-Boltzmann one [15]. We find that in this regime the QPT does not disappear and therefore the quantum fluctuations prevail upon the thermal ones (as can be seen in the noncommutative case in Fig. 1). Only in the limit of very high temperatures ( $\beta \rightarrow 0$ ) the QPT disappears.

The organization of the paper is as follows: in Sec. II we shall present the system to be analyzed and discuss the spectrum of the two phases, namely, the left and the right phase; in Sec. III, we present the method to calculate the partition function that characterizes the chiral phases at finite temperature and describes the phase transition as the strength of the magnetic field varies; in Sec. IV we scrutinize in details the magnetization at finite temperature and in Sec. VI we study the thermodynamic of a noncommutative Dirac Oscillator with a constant magnetic field. Finally, Sec. VII is devoted to conclusions.

## II. THE QUANTUM SYSTEM: DIRAC OSCILLATOR WITH A CONSTANT MAGNETIC FIELD

The non-relativistic version of the  $(2+1)$ -dimensional Dirac oscillator with a constant magnetic field and zero temperature can be associated to a chiral harmonic oscillator [7], that have been studied in [16]. Moreover, in [17, 18] a possible connection to topological Chern-Simons gauge theories has been pointed out. The case of the system presented in this paper can be seen as a relativistic extension of the chiral harmonic oscillators [7, 8], at finite temperature.

A relativistic spin-1/2 fermion constrained in a 2-dimensional plane with mass  $m$ , charge  $e$ , Dirac oscillator frequency  $\omega$  and subjected to a constant magnetic field orthogonal to the plane, is described by the Hamiltonian:

$$H = c \boldsymbol{\sigma} \cdot (\mathbf{p} - im\omega\sigma_z \mathbf{x} + \frac{e}{c} \mathbf{A}) + \sigma_z mc^2, \quad (1)$$

where  $c$  stands for the speed of light and  $\boldsymbol{\sigma} = (\sigma_x, \sigma_y)$ ,  $\sigma_z$  denotes the Pauli matrices. As in the usual notation, the  $\mathbf{p}$  and the  $\mathbf{x}$  represent the momentum and the position operators while the vector potential is related to the magnetic field through

$$\mathbf{A} = (-By/2, Bx/2). \quad (2)$$

This set-up offers an intriguing interplay: while the two-dimensional Dirac oscillator coupling endows the particle with an intrinsic left-handed chirality [3], the magnetic field coupling favors a right-handed chirality [2]. The interplay between opposed chirality interactions culminates in the appearance of a relativistic quantum phase transition, which can be fully characterized [7].

### A. Energy levels

In this section, we shall recall the spectrum and the degeneracy of the various energy levels of a two-dimensional relativistic Dirac oscillator in the two phases defined by  $B > B_{cr}$  and  $B < B_{cr}$ . The spectrum of the system is characterized by two quantum numbers:  $n_r = 0, 1, 2, \dots$ , the radial quantum number and  $M = 0, \pm 1, \pm 2, \dots$ , the 2-dimensional angular momentum quantum number.

In what we call the *left phase*, the energy level corresponding to the zero mode has positive energy  $E = mc^2$  and infinite degeneracy with respect to the non-negative magnetic quantum number  $M \geq 0$  (the negative magnetic numbers are forbidden [9]). The excited states are

$$E_N^\pm = \pm mc^2 \sqrt{1 + \xi_L N}, \quad (3)$$

$$N = n_r + \frac{|M| - M}{2}, \quad N = 1, 2, \dots \quad (4)$$

where  $N$  labels the energy levels,  $\xi_L$  is a constant encoding the parameters of the system that for the standard commutative case simply reads

$$\xi_L = -4X, \quad X := \frac{1}{mc^2} (\mu B - \hbar\omega) \quad (5)$$

and  $\mu = e\hbar/(2mc)$  denotes the Bohr magneton. The energy levels in (4) are degenerate. In particular, every level has infinite degeneracy, with respect to the non-negative values of  $M$ , and  $D = N + 1$  finite degeneracy with respect to the negative values of  $M$ .

The *right phase*, on the other hand, has zero mode degeneracy with respect to the non-positive magnetic quantum number  $M \leq 0$  and the value of the energy is in the negative branch:  $E = -mc^2$ . Similarly, the excited states have an infinite degeneracy with respect to non-positive values of  $M$ , while the degeneracy is  $D = N + 1$  with respect to  $M > 0$  and the energies read

$$E_N^\pm = \pm mc^2 \sqrt{1 + \xi_R N},$$

$$N = n_r + \frac{|M| + M}{2} \quad N = 1, 2, \dots, \quad (6)$$

where the parameter  $\xi_R$  is related to  $\xi_L$  by the relation  $\xi_R = -\xi_L$ . Note that, when  $\xi_R = \xi_L = 0$ , that is when

$$B = B_{cr} = \hbar\mu\omega, \quad (7)$$

all the energy levels collapse to the energy  $E = \pm mc^2$  and the *quantum phase transition* happens [7, 9].

### III. FINITE TEMPERATURE QUANTUM PHASE TRANSITION

To study the interplay between thermal and quantum fluctuations for this two-dimensional relativistic Dirac oscillator, we focus on the system at high temperatures when the electron-states statistics can be described with the Maxwell-Boltzmann statistics. We will show that in this regime the QPT will not disappear.

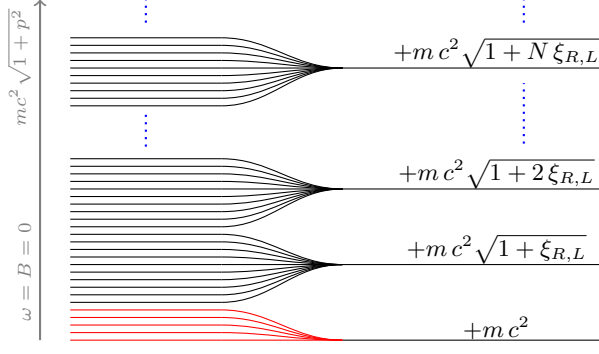


FIG. 2. Pictorial view of the positive branch of the energy levels that from a continuous spectrum for the free electron collapse to the discrete one in (4) and (6).

### A. Partition Function

The partition function for the positive branch of the energy levels (4) and (6) and the zero mode, has to take into account the degeneracy of each single energy level. Thus, it is defined by the product of the density of the states and the Boltzmann factor

$$Z_{L,R} = \sum_{M,n_r} \mathbf{g} e^{-\beta E_N^+}, \quad N = 0, 1, \dots, \quad (8)$$

where  $E_N^+$  are the values given by (4) and (6), and  $\beta$  is the inverse temperature.

To evaluate the density of the states  $\mathbf{g}$ , we can split every chiral phase of the system (left and right introduced in the previous section) into two different sub-systems with respect to the sign of the quantum number  $M$ .

If we consider a free electron with  $M > 0$  or alternatively  $M < 0$ , in a standard commutative spacetime and confined to a finite area  $L^2$ , the number of energy levels in the region  $dp_x dp_y$  around  $p_x$  and  $p_y$  is  $d\mathbf{g} = L^2 / (2h^2) dp_x dp_y$  [15]. Note that it can be proved that the phase-space volume element  $dp_x \wedge dp_y$  in the relativistic case is invariant for Lorentz transformations [19]. Moreover,  $L$  is the length in a rest-frame.

*a. Left Phase.* For  $M \geq 0$ , the degeneracy of each energy level (4) defined in the region  $\mathcal{K}$  of the momenta  $(p_x, p_y)$  such that  $E_N < E_{\text{free}}(p_x, p_y) < E_{N+1}$  (see Fig.2), where  $E_{\text{free}}$  is the energy of the free electron, is given by

$$\begin{aligned} \mathbf{g}_{M>0} &= \frac{1}{2} \left( \frac{L}{h} \right)^2 \iint_{\mathcal{K}} dp_x dp_y \\ &= \pi \left( \frac{L}{h} \right)^2 \left[ p^2 \right]_{\frac{p^2}{m^2 c^2} = \xi_L N}^{\frac{p^2}{m^2 c^2} = \xi_L (N+1)} = \left( \frac{Lmc}{h} \right)^2 \pi \xi_L(9) \end{aligned}$$

and  $N$  depends only on the quantum number  $n_r$  because the difference in (4) is zero. In the case  $M < 0$ , the number of levels collapsing into the level  $N$  is still equal to  $\mathbf{g}_{M>0}$ . However, one should consider that, when  $M < 0$ , as shown in (4),  $N$  depends on both the quantum

number  $M$  and  $n_r$ , namely  $N = n_r + M$ . Therefore, one needs to keep into account, for each energy level  $N$ , the degeneracy  $D$ , i.e.  $\mathbf{g}_{M<0} = \mathbf{g}_{M>0}/D$ . Thus, the number of states

$$\mathbf{g}_{M<0} = \left( \frac{Lmc}{h} \right)^2 \frac{\pi \xi_L}{(n_r - M + 1)}, \quad (10)$$

is not constant along the spectrum, but depends on the energy level.

Taking into account the degeneracy, using the spectrum (4) and its zero point energy, the partition function with Boltzmann statistics of the states of a single oscillator<sup>1</sup> for the left phase is

$$\begin{aligned} Z_L &= \left( \frac{Lmc}{h} \right)^2 \pi \xi_L \left[ e^{-\beta mc^2} + \sum_{n_r=1}^{\infty} e^{-\beta mc^2 \sqrt{1+\xi_L n_r}} + \right. \\ &\quad \left. + \sum_{n_r=1}^{\infty} \sum_{M=0}^{-\infty} \frac{e^{-\beta mc^2 \sqrt{1+\xi_L (n_r-M)}}}{(n_r - M + 1)} \right]. \quad (11) \end{aligned}$$

Notice that the contribution to the partition function of the zero mode energy appears only for  $M \geq 0$  [9] and, as we will see later in sec. III C, this will be the source of the non-analyticity of the partition function at the phase point. The sum in the third term of (11) coincides with the second if we introduce  $M'$  and  $N'$  such that  $M' = -M$  then  $n_r + M' = N'$ , obtaining

$$\sum_{n_r=1}^{\infty} \sum_{N'=n_r}^{\infty} \frac{e^{-\beta mc^2 \sqrt{1+\xi_L (N')}}}{(N' + 1)} = \sum_{N'=1}^{\infty} e^{-\beta mc^2 \sqrt{1+\xi_L (N')}} \quad (12)$$

so, over all, the two sectors ( $M > 0$  and  $M < 0$ ) equally contribute to the partition function.

*b. Right Phase* The partition function for the right phase, defined by the energy levels (6), is equal to (11) except for the zero mode term. This is because, as explained in Sec. II, the zero mode contributes only to the negative energies branch.

### B. Zeta-function representation

A different representation of the defining series in the partition function that will reveal itself to be more effective when the phase switches from left to right, can be obtained using the Cahen-Mellin integral, as suggested for different systems in [20] and reviewed in [21, 22]. The Cahen-Mellin integral is defined as [23]

$$e^{-x} = \frac{1}{2\pi i} \int_{c-i\infty}^{c+i\infty} \Gamma(s) x^{-s} ds \quad \left( |\arg x| < \frac{1}{2}\pi; x \neq 0 \right) \quad (13)$$

<sup>1</sup> The classical multi-oscillator states partition function is simply  $(Z_L)^n / n!$  for  $n$  electrons [15].

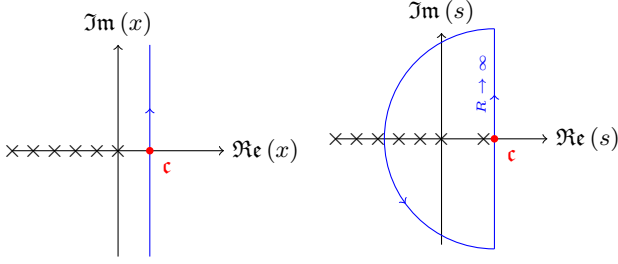


FIG. 3. (Left) Poles of the argument of the Cahlen-Mellin integral (13). (Right) Path in the complex plane over which the contour integration (16) is performed. The semicircle of radius  $R \rightarrow \infty$  is closed on the left.

where  $\mathbf{c}$  is real and  $\mathbf{c} > 0$ . The argument of the integral has poles for all  $x = -n$ ,  $n \in \mathbb{N}_0$  and the residuals at the negative poles are  $(-1)^n/n!$  (see Fig. 3). Using (13) to calculate the second term in the partition function (11) and including the sum into the integral, we have that the term

$$\xi_L \sum_{n_r=1}^{\infty} e^{-\beta m c^2 \sqrt{1+\xi_L n_r}} \quad (14)$$

can be rewritten as

$$\frac{\xi_L}{2\pi i} \int_{\mathbf{c}-i\infty}^{\mathbf{c}+i\infty} \frac{\Gamma(s)}{(\beta m c^2)^s} \sum_{n_r=1}^{\infty} \frac{1}{(1+\xi_L n_r)^{s/2}} ds. \quad (15)$$

The series in (15) can be recognized as the series representation of the Hurwitz- $\zeta$  function  $\zeta(v, a) = \sum_{n=0}^{\infty} \frac{1}{(n+a)^v}$  that converges only if  $\Re(v) > 1$ . Under this condition the integral (15) becomes

$$\frac{\xi_L}{2\pi i} \int_{\mathbf{c}-i\infty}^{\mathbf{c}+i\infty} \frac{\Gamma(s)}{(\beta m c^2 \xi_L^{1/2})^s} \zeta\left(\frac{s}{2}, \frac{1}{\xi_L} + 1\right) ds. \quad (16)$$

In contrast to what has been proposed in the recent literature on the topic (see [22] and references therein), we notice that the condition for the convergence of the series  $s/2 > 1$  implies  $\mathbf{c} > 2$ . The integral can therefore be evaluated with the method of residue once a proper closed path has been identified. Because of the presence of the  $\Gamma$ -function that diverges as  $\Gamma(s) = (2\pi)^{1/2} e^{-s} s^{s-1/2} [1 - \mathcal{O}(s^{-1})]$ , the integration in (16) can be closed only on the left part of the complex plane, allowing to use the Cauchy's residue theorem on the poles  $\{s = 2, 0, \mathbb{Z}^-\}$  represented in Fig. 3. Introducing the adimensional variable  $\tilde{\beta} = \beta m c^2$ , the partition

functions for both the phases becomes

$$Z_{L,R} = 2\pi \left(\frac{Lmc}{h}\right)^2 \times \left[ \left(\frac{2}{\tilde{\beta}^2} - 1\right) + \left(\frac{\Theta e^{-\tilde{\beta}}}{2} - \frac{1}{2}\right) \xi_{L,R} + \sum_{n=1}^{\infty} \frac{(-\tilde{\beta})^n \xi_{L,R}^{\frac{n}{2}+1}}{n!} \zeta\left(-\frac{n}{2}, 1 + \frac{1}{\xi_{L,R}}\right) \right], \quad (17)$$

where now we use the subscript  $L, R$  to indicate both the left and right phase and  $\Theta$  is a step function that is equal to zero (one) for the right phase (left phase). This series representation can be seen as a series expansion in power of  $\beta$ , namely a high-temperature power expansion. From now on the quantity in the square brackets of (17) will be called  $\tilde{Z}_{L,R}$

$$Z_{L,R} = 2\pi \left(\frac{Lmc}{h}\right)^2 \tilde{Z}_{L,R}. \quad (18)$$

The series representations of the partition function  $\tilde{Z}_{L,R}$  in terms of the  $\zeta$ -function and the Boltzmann representation introduced in (11) can be both evaluated numerically considering only a finite number of terms in the series. However, the Boltzmann representation encounters obvious numerical issues for small values of  $\xi_{L,R}$ , i.e. close to the value where the phase transition happens. These issues do not affect the  $\zeta$ -function representation of the partition function and, as we will see in the next subsection, the partition function can be evaluated analytically for small values of  $\xi_{L,R}$ . Fig. 4 shows  $\tilde{Z}_{L,R}$  in the  $\zeta$ -function representation keeping  $n_{\max} = 100$  terms of the series in (17).

### C. Partition function near the critical point

The partition function (17) can be used to calculate the asymptotic expansion near the critical point, namely when  $\xi_{L,R} \rightarrow 0$ . This allows to analytically explore the regimes close to the phase transition and study the interplay between thermal and quantum fluctuations. The asymptotic expansion of the Hurwitz- $\zeta$  function [24, 25] is

$$\zeta(s, a) = \frac{a^{1-s}}{s-1} + \frac{1}{2} a^{-s} + \frac{Z(s, a)}{\Gamma(s)} \quad (19)$$

where the large- $a$  (Poincaré) asymptotic expansion of the function  $Z(s, a)$

$$Z(s, a) \sim \sum_{k=1}^{\infty} \frac{B_{2k}}{(2k)!} \frac{\Gamma(2k + s - 1)}{a^{2k+s-1}}, \quad |a| \rightarrow \infty \quad (20)$$

is valid in  $|\arg a| < \pi$  and  $B_{2k}$  denote the even-order Bernoulli numbers. Writing explicitly the sum (20) in

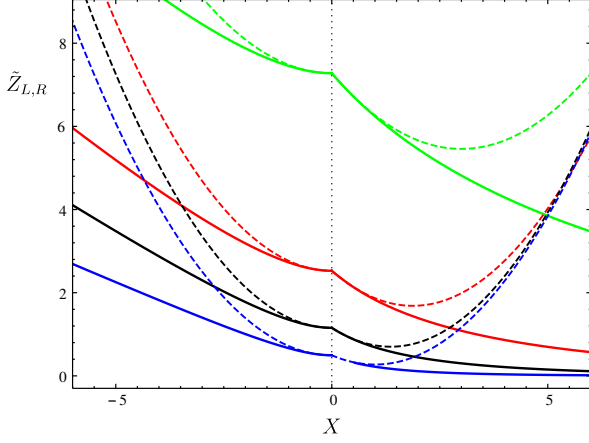


FIG. 4. Scaled partition function for the commutative Dirac oscillator and its second order approximation at the critical point (dashed) as a function of the scaled effective magnetic energy  $X$ , defined in (5), for different values of the temperature:  $\tilde{\beta} = 0.5, 0.8, 1.1, 1.5$  respectively green, red, black and blue lines.

the partition function  $\tilde{Z}_{L,R}$  gives

$$\begin{aligned} \tilde{Z}_{L,R} &= \frac{2}{\tilde{\beta}^2} - 1 - \left(1 - \Theta e^{-\tilde{\beta}}\right) \frac{\xi_{L,R}}{2} + \\ &+ \sum_{n=1}^{\infty} \frac{(-\tilde{\beta})^n}{n!} \left\{ \left[ \frac{1}{2} \xi_{L,R} - \frac{2(\xi_{L,R} + 1)}{n+2} \right] (\xi_{L,R} + 1)^{\frac{n}{2}} + \right. \\ &\left. + \sum_{k=1}^{\infty} \frac{B_{2k}}{(2k)!} \frac{\Gamma(2k - \frac{n}{2} - 1)}{\Gamma(-\frac{n}{2})} \frac{\xi_{L,R}^{2k}}{(\xi_{L,R} + 1)^{2k - \frac{n}{2} - 1}} \right\}. \quad (21) \end{aligned}$$

Using the binomial series and the relation between Euler gamma functions

$$\Gamma\left(-\frac{n}{2}\right) \Gamma\left(1 + \frac{n}{2}\right) = \frac{\pi}{\sin(-\pi n/2)}, \quad (22)$$

one can rewrite the terms in the curly brackets in (21) as

$$\begin{aligned} \sum_{w=0}^{\infty} \frac{1}{w!} \left\{ \left[ \frac{1}{2} \xi_{L,R} - \frac{2(\xi_{L,R} + 1)}{n+2} \right] \frac{\Gamma(1 + \frac{n}{2})}{\Gamma(1 + \frac{n}{2} - w)} \xi_{L,R}^w + \right. \\ \left. + \sum_{k=1}^{\infty} \frac{B_{2k}}{(2k)!} \frac{\Gamma(1 + \frac{n}{2})}{\Gamma(-2k + \frac{n}{2} + 2 - w)} \xi_{L,R}^{2k+w} \right\} \quad (23) \end{aligned}$$

defining in this way the partition function at all orders in  $\xi_{L,R}$  near the critical point. At the second order in  $\xi_{L,R}$ , one can sum the partition function at all orders in  $\tilde{\beta}$ , so that, near the critical point, it reads

$$\begin{aligned} \tilde{Z}_{L,R} &= \frac{2e^{-\tilde{\beta}}}{\tilde{\beta}} \left[ 1 + \frac{1}{\tilde{\beta}} + (\Theta - 1) \frac{\tilde{\beta} \xi_{L,R}}{4} + \frac{\tilde{\beta}^2 \xi_{L,R}^2}{48} \right] + \\ &+ \mathcal{O}(\xi_{L,R}^3). \quad (24) \end{aligned}$$

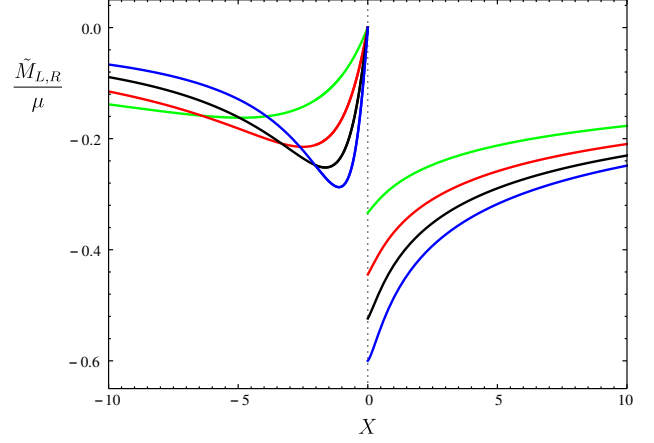


FIG. 5. Scaled magnetization of the commutative Dirac oscillator as function of the scaled effective magnetic energy  $X$ , defined in (5), for different values of the temperature  $\tilde{\beta} = 0.5, 0.8, 1.1, 1.5$  respectively green, red, black and blue lines.

This expression is a continuous but non-analytic function in  $\xi_{L,R}$  and, in fact,  $\Theta$  brings a discontinuity in the first order derivatives. The function to the second order (24) is compared with (17) in Fig. 4.

#### IV. MAGNETIZATION AT FINITE TEMPERATURE

At this point, it is possible to use the derived expression for the partition function (17) to calculate a physical observable quantity like the magnetization [26, 27]. Indeed, in [9] the magnetization has been proposed as the quantity able to distinguish between the phases of the system.

The magnetization for a system at finite temperature, can be defined as [15]

$$M = k_B T \frac{\partial \log Z}{\partial B} = \frac{1}{\beta Z} \frac{\partial Z}{\partial \xi} \frac{\partial \xi}{\partial X} \frac{\partial X}{\partial B}. \quad (25)$$

In order evaluate the derivative  $\partial Z / \partial \xi_{L,R}$  one can use in (17) the following identity [28]

$$\frac{\partial \zeta(s, a)}{\partial a} = -s \zeta(s+1, a) \text{ for } s \neq 0, 1 \Re a > 0. \quad (26)$$

The magnetization evaluated numerically with  $n_{\max} = 60$  is illustrated in Fig. 5. Interestingly, we find that the magnetization in the left phase, has opposite sign with respect to the single state result obtained at  $T = 0$  [9]. At finite temperature, in  $\xi_L = \xi_R = 0$  the magnetization manifests a discontinuity.

Analogously to what has been done for the partition function in the previous sections, we now inspect the magnetization behaviour at values of the magnetic field close to the critical values. To approximate the full partition function in the neighborhood of  $\xi_L = \xi_R = 0$ , we

can either follow the steps described in subsection III C for the full partition function resulting of (25), or we can use (24) in (25).

At the critical point, the magnetization is not a continuous function of the magnetic field and can be written as a series expansion around  $X = 0$  at all order in  $\beta$  as

$$\begin{aligned} \frac{M_{R,L}}{\mu} &= -\frac{\tilde{\beta}}{\tilde{\beta}+1}H(X) + \\ &+ \left(\frac{\tilde{\beta}}{\tilde{\beta}+1}\right)^2 \left[\frac{2}{3} + \tilde{\beta}\left(H(-X) - \frac{1}{3}\right)\right] X + \mathcal{O}(X^2), \end{aligned} \quad (27)$$

where  $H(x)$  is the Heaviside step function. The discontinuity with respect to the magnetic field at the critical point  $X = 0$  is

$$|\Delta M_{\text{cr}}| = \mu \frac{\tilde{\beta}}{(1+\tilde{\beta})}. \quad (28)$$

In the limit  $\tilde{\beta} \rightarrow 0$ , the thermal fluctuations overcome the quantum ones, the gap disappears and the magnetization is zero for both the chiralities.

## V. OTHER THERMODYNAMIC FUNCTIONS

Once the partition function has been calculated, the thermodynamics of the system can be fully explored. Using

$$\begin{aligned} F &= -\frac{1}{\beta} \ln Z, & U &= -\frac{\partial}{\partial \beta} \ln Z, \\ S &= k_B \beta^2 \frac{\partial F}{\partial \beta}, & C &= -k_B \beta^2 \frac{\partial U}{\partial \beta}, \end{aligned} \quad (29)$$

in Fig. 6, we plot the thermodynamic quantities for the commutative system. The specific heat as function of the  $\beta$  manifests a non-monotonic behaviour in the left phase, while it becomes monotonic in the right phase.

## VI. NONCOMMUTATIVE DIRAC OSCILLATOR WITH A CONSTANT MAGNETIC FIELD

In the previous sections we described the Dirac oscillator under a uniform magnetic field and its associated QPT in a 2D space-time. Now, we move to the noncommutative system, indeed, studies in quantum gravity and string theory propose that the space-time can be fundamentally or effectively described by a generalization of geometry where, locally, coordinates do not necessarily commute [29–39]. Moreover, recent developments in condensed matter physics, suggest the use of the noncommutative geometry framework to encode geometrical properties of topological quantum systems [40–43].

The study of the Dirac oscillator in the presence of noncommutative coordinates and momenta and a constant magnetic field in a 2-dimensional space at zero-temperature has been carried out in [9]. The system that in the commutative case undergoes a quantum phase transition at finite magnetic field, also exhibits in the noncommutative case another phase transition at a higher magnetic field. The third region appears to have the same chirality of the first one providing a re-entrant quantum phase transition [10].

In this section, we will study the noncommutative system at finite temperature, the parametrization that has been used for the exact calculation of the spectrum in [9] will allow us to exploit all the calculation done in the previous sections and easily study the QPTs in the noncommutative space.

### A. Energy levels

The Hamiltonian for the (2 + 1)-dimensional Dirac oscillator in the noncommutative plane with a homogeneous magnetic field can be written in a way similar to (1)

$$\hat{H} = c\boldsymbol{\sigma} \cdot (\hat{\mathbf{p}} - im\omega\sigma_z\hat{\mathbf{x}} + \frac{e}{c}\hat{\mathbf{A}}) + \sigma_z mc^2, \quad (30)$$

where now the *hat* indicates the noncommutative operators. In this framework, the commutation relation between coordinates and momenta are given by [29]

$$[\hat{x}, \hat{y}] = i\theta, \quad [\hat{p}_x, \hat{p}_y] = i\eta, \quad [\hat{x}_i, \hat{p}_j] = i\hbar(1 + \frac{\theta\eta}{4\hbar^2})\delta_{ij}, \quad (31)$$

where  $\theta, \eta \in \mathbb{R}$ . The noncommuting coordinates and momenta can be expressed in terms of commuting ones using the Seiberg-Witten map and are given by

$$\begin{aligned} \hat{x} &= x - \frac{\theta}{2\hbar}p_y, & \hat{p}_x &= p_x + \frac{\eta}{2\hbar}y, \\ \hat{y} &= y + \frac{\theta}{2\hbar}p_x, & \hat{p}_y &= p_y - \frac{\eta}{2\hbar}x. \end{aligned} \quad (32)$$

The Hamiltonian (30) can be rewritten as

$$H = c \begin{pmatrix} mc & \hat{\Pi}_- \\ \hat{\Pi}_+ & -mc \end{pmatrix}, \quad (33)$$

where  $\hat{\Pi}_{\pm}$  are given by

$$\begin{aligned} \hat{\Pi}_{\pm} &= \left(1 - \frac{\tilde{\omega} - \omega}{\omega\theta}\right) (p_x \pm ip_y) \pm \\ &\pm im(\tilde{\omega} - \omega - \omega_\eta)(x \pm iy) \end{aligned} \quad (34)$$

after introducing the following frequencies out of the parameters of the system:

$$\tilde{\omega} = \frac{eB}{2mc}, \quad \omega_\theta = \frac{2\hbar}{m\theta}, \quad \omega_\eta = \frac{\eta}{2\hbar m}. \quad (35)$$

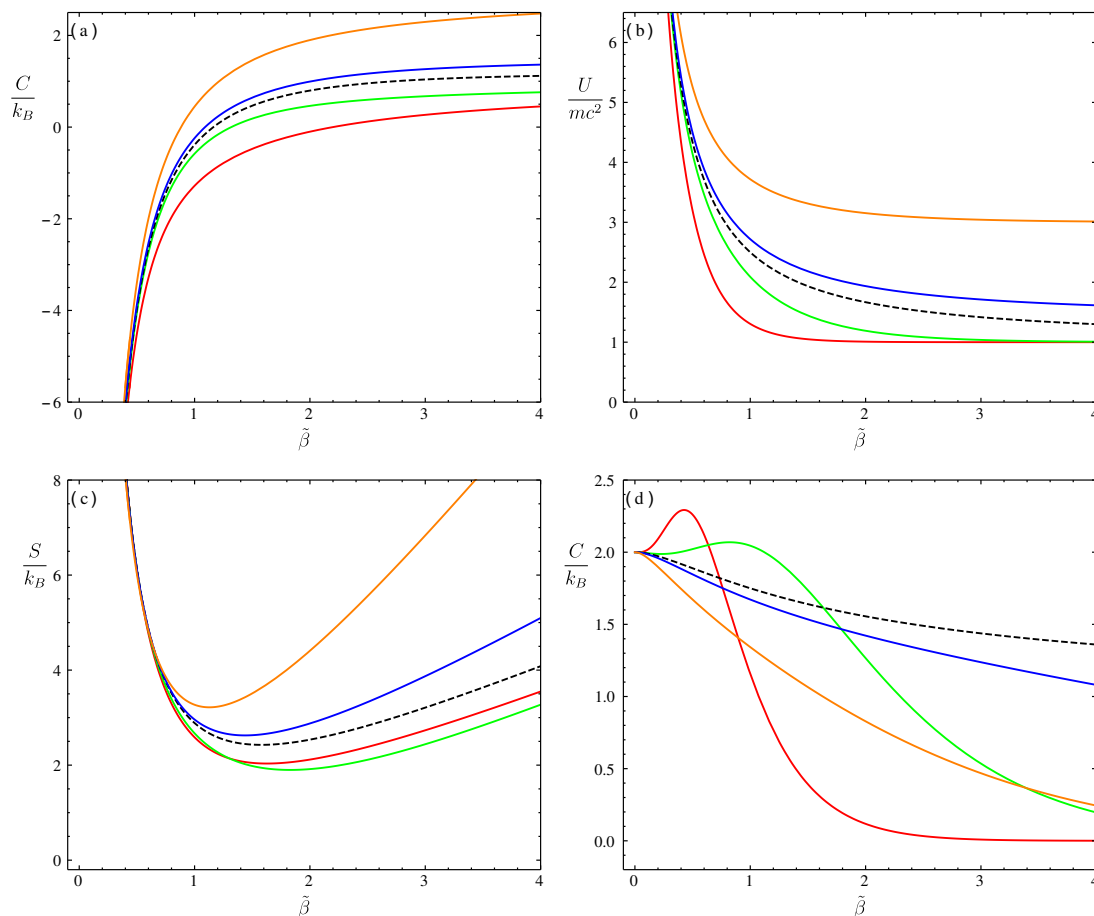


FIG. 6. Various thermodynamic functions versus the scaled inverse temperature  $\tilde{\beta} = mc^2/k_B T$  for different values of the magnetic field, corresponding to  $X = -4.5, -1.3, 0, 0.3, 2$  respectively red, green, dashed-black, blue, orange. The  $X = 0$  case (dashed black) represents the critical value of the magnetic field. Upper left panel (a): the free energy  $F/mc^2$ ; upper right panel (b): the internal energy  $U/mc^2$ ; lower left (c): the entropy  $S/k_B$  and finally in the lower right panel (d) the specific heat  $C/k_B$ . In the last one, it is visible the difference between the red and green (left phase) and the blue and orange (right phase).

With this parametrization it is clear that there are two critical values of the magnetic field

$$B_{\text{cr}} = \frac{2mc}{e}(\omega + \omega_\eta) = \frac{2c}{e}\left(m\omega + \frac{2\eta}{\hbar}\right), \quad (36)$$

$$B_{\text{cr}}^* = \frac{2mc}{e}(\omega + \omega_\theta) = \frac{2c}{e}\left(m\omega + \frac{\hbar}{\theta}\right). \quad (37)$$

such that for both  $B = B_{\text{cr}}$  and  $B = B_{\text{cr}}^*$ , there are no interactions in the model and the Hamiltonian represents a free particle (only kinetic energy). Since the critical value  $B_{\text{cr}}$  depends on the momentum noncommutative parameter  $\eta$ , this shifts the value of the critical field relative to the value in (7). The space noncommutativity ( $\theta \neq 0$ ) instead introduces the additional critical value for the magnetic field ( $B_{\text{cr}}^*$ ) [9].

Interestingly, the parameters used in the noncommutative massive Dirac oscillator can be re-absorbed in such a way that one can study the single phases independently. In fact, the behaviour of the single phases can be described regardless of the parameters encoding the noncommutative physics [9]. Therefore, although

the noncommutative system has two more parameters, they can recast into the parameter  $\xi_{L,R}$  allowing us to use most of the calculations performed in the previous sections for the commutative case. The main difference now is that the magnetic field and the noncommutative parameters are related by

$$\xi_L = -4 \frac{mc^2}{\omega_\theta \hbar} \left( \frac{\omega_\theta \hbar}{mc^2} - X \right) \left( X - \frac{\omega_\eta \hbar}{mc^2} \right) \quad (38)$$

while it is still valid the relation  $\xi_R = -\xi_L$ . Phase changes occur at critical values of the magnetic field that makes the parameter  $\xi_{L,R}$  null. Note that, differently from the commutative case (5), in the noncommutative case the equation (38) is quadratic in  $B$  and consequently it admits two critical points.

## B. Energy levels and partition function

In Section II A we reviewed the spectrum of the system as a function of the parameter  $\xi_{L,R}$ . As mentioned

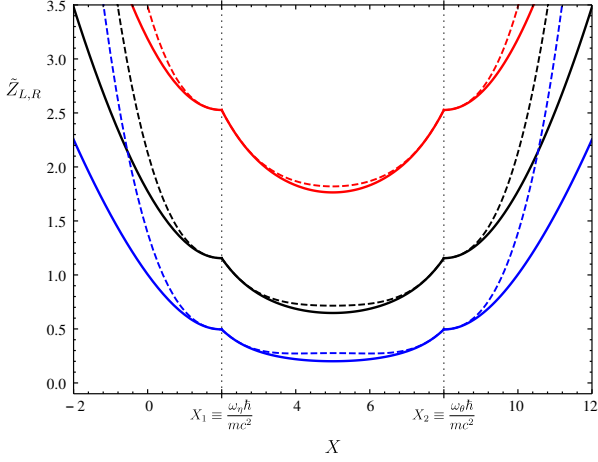


FIG. 7. Scaled partition function in the noncommutative case and its approximation near the critical points  $X_1$ ,  $X_2$  (dashed) with  $X_1 = \omega_\eta \hbar / mc^2 = 2$ ,  $X_2 = (\omega_\theta \hbar / mc^2) = 8$  and  $\tilde{\beta} = 0.8, 1.1, 1.5$  for respectively red, black and blue lines.

above, for the noncommutative case, the spectrum remains equal to (4) and (6) as a function of the parameter  $\xi_{L,R}$  that now becomes (38), quadratic in  $B$ . Since the density of the energy states is also a function of the parameters  $\xi_{L,R}$ , its contribution to the partition function of each energy level in the noncommutative case coincides with the one in the commutative case (10). The resulting partition function is illustrated in Fig. 7. In the plot is also represented the outcome of the approximation once the constant  $\xi_{L,R}$  in (38) is replaced in (24). The partition function can be used to calculate the other thermodynamic quantities using (29). In particular, the heat capacity is shown in Fig. 1. In [44] a different noncommutative model has been studied without considering the degeneracy of the states.

### C. Magnetization

The magnetization for the noncommutative Dirac oscillator case is illustrated in Fig. 8. The figure shows the presence of a fixed point at  $M = 0$  for every  $T$ . The point where the magnetization changes its sign appears only in the noncommutative case and is a consequence of the term  $\partial \xi / \partial X$  in (25), that is a non constant function of  $X$ :

$$\begin{aligned} \frac{\partial \xi_{L,R}}{\partial X} &= \pm 4 \frac{mc^2}{\omega_\theta \hbar} \left[ 2X - \frac{\hbar(\omega_\eta + \omega_\theta)}{mc^2} \right] = \\ &= \pm 4 \sqrt{\frac{m c^2}{\hbar \omega_\theta} \xi_{L,R} \pm \frac{(\omega_\eta - \omega_\theta)^2}{\omega_\theta^2}} \end{aligned} \quad (39)$$

where the plus sign is for the  $L$  phase and the minus sign is for the  $R$  phase. From the first line of (39), we find that at the point  $X_0 = \frac{\hbar(\omega_\eta + \omega_\theta)}{2mc^2}$  the magnetization

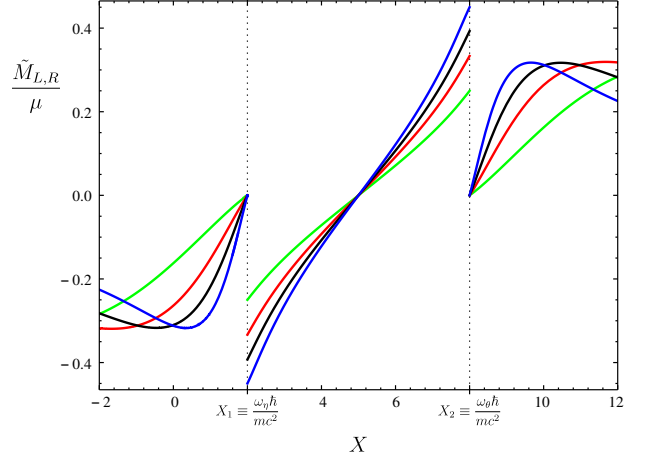


FIG. 8. Scaled magnetization in the noncommutative case as function of the scaled effective magnetic energy  $X$ , defined in (5), for different values of the rescaled inverse temperature  $\tilde{\beta} = 0.5, 0.8, 1.1, 1.5$  respectively green, red, black and blue lines. The parameters are fixed as in Fig. 7.

changes sign. Therefore, the point where the magnetization smoothly vanishes is the midpoint between the two critical points. This feature of the noncommutative system is independent of the temperature and was also present in the analysis at  $T = 0$  [9]. Near the critical point, we can evaluate the magnetization in  $\xi_{L,R}$  using the second line of (39) and (24) in (25), obtaining:

$$\frac{\partial \xi_{L,R}}{\partial X} = \pm 4 \left[ \left| \frac{(\omega_\eta - \omega_\theta)}{\omega_\theta} \right| \pm \frac{1}{2} \frac{m c^2}{\hbar} \frac{\xi_{L,R}}{|\omega_\eta - \omega_\theta|} + \mathcal{O}(\xi^2) \right], \quad (40)$$

and the other terms in (25) read

$$\begin{aligned} \frac{1}{\tilde{\beta}} \frac{1}{Z} \frac{\partial Z}{\partial \xi} &= \frac{\tilde{\beta}}{4(\tilde{\beta} + 1)} (\Theta - 1) + \\ &+ \left[ \frac{\tilde{\beta}}{4(\tilde{\beta} + 1)} \right]^2 \left[ \frac{2}{3} + \tilde{\beta} \left( \Theta - \frac{1}{3} \right) \right] \xi + \mathcal{O}(\xi^2). \end{aligned} \quad (41)$$

Then the discontinuity of the magnetization at the two critical points, for the noncommutative case is

$$\Delta M = \pm \mu \left| \frac{(\omega_\eta - \omega_\theta)}{\omega_\theta} \right| \frac{\tilde{\beta}}{(\tilde{\beta} + 1)}, \quad (42)$$

and we can notice that if  $\eta$ , the noncommutative parameter related with the momenta, vanishes then the transitions become independent from  $\theta$ , the coordinates noncommutative parameter.

## VII. CONCLUSIONS

Over the years, the Dirac oscillator has become a valuable tool for various branches of physics, mostly because



it is one of the few relativistic systems whose exact solutions are known. The  $(2 + 1)$ -dimensional case, namely when an electron is constrained to live in a plane, manifests an intrinsic chiral behavior of its states. An external magnetic field interacts at the quantum level with the chirality properties of the system and, if strong enough, it forces an abrupt switch in the electron chirality. This behavior studied at zero temperature, distinguish two phases of the electron at different regimes, and their change is recognized to be a quantum phase transition [7]. Magnetization shows a discontinuity at a finite value of the magnetic field [9]. The quantum nature of this behavior raises the question on how thermal fluctuations interacts with the system and when the thermal disorder destroys these quantum effects. In this paper, we analyze the interplay between these two physical phenomena. In particular, we quantify the discontinuity of the magnetization of the QPT at finite temperature  $\Delta M \propto \hbar \left[ \frac{1}{k_B T} + O\left(\frac{1}{k_B T}\right)^2 \right]$ . This discontinuity is a quantum phenomenon that tends to zero for high temperatures. While the critical values of the system are not affected by changes in temperature, we noticed a crucial difference from the system at  $T = 0$  studied in [9]: the magnetization at finite temperature has regimes with opposite sign with respect to the single state (zero-temperature) case. This opens to the possibility of a second phase transition at low temperatures, where the statistics of the states becomes quantum and cannot be described by Boltzmann statistics. In Fig. 6 we report various thermodynamic quantities that can be evaluated once the partition function is provided. The specific heat shows different behaviors at different phases of the system.

The series representations of the partition function proposed in this paper allow to explore the system in diverse regimes: far, close and at the critical points. The representation in terms of the Hurwitz-zeta function fixes some misunderstandings present in the litera-

ture regarding which poles play a role in the evaluation of the partition function.

We also generalize our calculations to the Dirac oscillator in noncommutative momenta and coordinates. The interest for this system comes from the fact that at zero temperature it manifests a re-entrant quantum phase transition, that we find is present also at finite temperature. Interestingly, there are systems in condensed matter physics that in certain regimes appear to have behavior similar and some times mathematically equivalent to systems living in a noncommutative space-time [40–43]. This opens the avenue of an *analogue non-commutativity* that is the possibility of studying, also experimentally, systems that are mathematically equivalent to those with noncommuting coordinates and/or momenta but are condensed matter systems living in an ordinary commutative space. The “analogue” approach to theoretical models that are too extreme or too weak to be measured directly has already been successfully employed in high-energy physics, and in particular in gravity with the so called analogue gravity [45]. This program is in constant development and already lead to important successes such as the measures of the analogue Hawking radiation [46–49], phenomenon that seemed to be only a theoretical model. It is interesting and challenging to find an analogue system that would allow the experimental measure of the re-entrant phase transition described in this paper, and we leave it for future investigation.

## ACKNOWLEDGEMENTS

A.M.F. would like to thank the Stiftung Giersch for the generous support during this work. D.M. acknowledges L. Malagò for discussions and support.

- 
- [1] S. Sachdev, *Quantum Phase Transitions*, 2nd ed. (Cambridge University Press, 2011).
  - [2] A. Bermudez, M. A. Martin-Delgado, and E. Solano, *Phys. Rev. Lett.* **99**, 123602 (2007).
  - [3] A. Bermudez, M. A. Martin-Delgado, and E. Solano, *Physical Review A* **76**, 041801 (2007), [arXiv:0704.2315 \[quant-ph\]](#).
  - [4] A. Bermudez, M. A. Martin-Delgado, and A. Luis, *Phys. Rev. A* **77**, 033832 (2008).
  - [5] B. P. Mandal and S. Verma, *Phys. Lett.* **A374**, 1021 (2010), [arXiv:0907.4544 \[hep-th\]](#).
  - [6] B. P. Mandal and S. K. Rai, *Phys. Lett.* **A376**, 2467 (2012), [arXiv:1203.2714 \[hep-th\]](#).
  - [7] A. Bermudez, M. A. Martin-Delgado, and A. Luis, *Physical Review A* **77**, 063815 (2008), [arXiv:0802.0577 \[quant-ph\]](#).
  - [8] C. Quimbay and P. Strange, (2013), [arXiv:1312.5251 \[quant-ph\]](#).
  - [9] O. Panella and P. Roy, *Phys. Rev.* **A90**, 042111 (2014), [arXiv:1409.5077 \[hep-th\]](#).
  - [10] O. Panella and P. Roy, *Journal of Physics: Conference Series* **670**, 012040 (2016).
  - [11] C. S. Hudson, *Zeitschrift für Physikalische Chemie* **47**, 113 (1904).
  - [12] R. B. Mann, “The chemistry of black holes,” in *1st Karl Schwarzschild Meeting on Gravitational Physics*, edited by P. Nicolini, M. Kaminski, J. Mureika, and M. Bleicher (Springer International Publishing, Cham, 2016) pp. 197–205.
  - [13] N. Altamirano, D. Kubiznak, and R. B. Mann, *Phys. Rev.* **D88**, 101502 (2013), [arXiv:1306.5756 \[hep-th\]](#).
  - [14] A. M. Frassino, D. Kubiznak, R. B. Mann, and F. Simovic, *JHEP* **09**, 080 (2014), [arXiv:1406.7015 \[hep-th\]](#).
  - [15] R. Kubo, H. Ichimura, T. Usui, and N. Hashitsume, *Statistical Mechanics (North-Holland Personal*

- Library*), 1st ed. (North Holland, 1990).
- [16] R. Banerjee and S. Ghosh, *J. Phys.* **A31**, L603 (1998), [arXiv:quant-ph/9805009 \[quant-ph\]](#).
- [17] M. M. Horta Barreira and C. Wotzasek, *Phys. Rev.* **D45**, 1410 (1992).
- [18] G. V. Dunne, R. Jackiw, and C. A. Trugenberger, *Phys. Rev.* **D41**, 661 (1990).
- [19] R. Hakim, *Introduction to Relativistic Statistical Mechanics: Classical and Quantum* (World Scientific, 2011).
- [20] I. H. Brevik, R. Herikstad, and S. Skriudalen, *Int. J. Mod. Phys.* **D16**, 1273 (2007), [arXiv:hep-th/0508123 \[hep-th\]](#).
- [21] M.-A. Dariescu and C. Dariescu, *Chaos, Solitons & Fractals* **33**, 776 (2007).
- [22] A. Boumali, *EJTP* **12**, 121 (2015), [arXiv:1409.6205 \[quant-ph\]](#).
- [23] R. B. Paris and D. Kaminski, *Asymptotics and Mellin-Barnes Integrals (Encyclopedia of Mathematics and its Applications)*, 1st ed. (Cambridge University Press, 2001).
- [24] R. B. Paris, *Proc. R. Soc. Lond. Ser. A Math. Phys. Eng. Sci.* **461**, 297 (2005), [arXiv:1407.2782 \[math.CA\]](#).
- [25] W. Magnus, F. Oberhettinger, and R. SONI, *Formulas and Theorems for the Special Functions of Mathematical Physics*, Grundlehren der mathematischen Wissenschaften (Springer Berlin Heidelberg, 2013).
- [26] D. Yoshioka and H. Fukuyama, *Journal of the Physical Society of Japan* **61**, 2368 (1992), [arXiv:cond-mat/9904052](#).
- [27] J. O. Andersen and T. Haugset, *Phys. Rev.* **D51**, 3073 (1995), [arXiv:cond-mat/9410084 \[cond-mat\]](#).
- [28] DLMF, “NIST Digital Library of Mathematical Functions,” <http://dlmf.nist.gov/>, Release 1.0.10 of 2015-08-07, online companion to [50].
- [29] O. Bertolami, J. G. Rosa, C. M. L. de Aragao, P. Castorina, and D. Zappala, *Phys. Rev.* **D72**, 025010 (2005), [arXiv:hep-th/0505064 \[hep-th\]](#).
- [30] J. Gamboa, M. Loewe, F. Mendez, and J. C. Rojas, *Int. J. Mod. Phys.* **A17**, 2555 (2002), [arXiv:hep-th/0106125 \[hep-th\]](#).
- [31] D. Itô, K. Mori, and E. Carriere, *Il Nuovo Cimento A (1965-1970)* **51**, 1119 (1967).
- [32] S. Bellucci, A. Nersessian, and C. Sochichiu, *Phys. Lett.* **B522**, 345 (2001), [arXiv:hep-th/0106138 \[hep-th\]](#).
- [33] C. Duval and P. A. Horvathy, *Phys. Lett.* **B479**, 284 (2000), [arXiv:hep-th/0002233 \[hep-th\]](#).
- [34] J. Gamboa, M. Loewe, F. Mendez, and J. C. Rojas, *Mod. Phys. Lett.* **A16**, 2075 (2001), [arXiv:hep-th/0104224 \[hep-th\]](#).
- [35] J. Gamboa, M. Loewe, and J. C. Rojas, *Phys. Rev.* **D64**, 067901 (2001), [arXiv:hep-th/0010220 \[hep-th\]](#).
- [36] P. A. Horvathy, L. Martina, and P. C. Stichel, *SIGMA* **6**, 060 (2010), [arXiv:1002.4772 \[hep-th\]](#).
- [37] V. P. Nair and A. P. Polychronakos, *Phys. Lett.* **B505**, 267 (2001), [arXiv:hep-th/0011172 \[hep-th\]](#).
- [38] A. Smailagic and E. Spallucci, *Phys. Rev.* **D65**, 107701 (2002), [arXiv:hep-th/0108216 \[hep-th\]](#).
- [39] A. Smailagic and E. Spallucci, *J. Phys.* **A35**, L363 (2002), [arXiv:hep-th/0205242 \[hep-th\]](#).
- [40] T. Neupert, L. Santos, S. Ryu, C. Chamon, and C. Mudry, *Phys. Rev. B* **86**, 035125 (2012), [arXiv:1202.5188 \[cond-mat.str-el\]](#).
- [41] F. D. M. Haldane, *Phys. Rev. Lett.* **107**, 116801 (2011), [arXiv:1106.3375 \[cond-mat.mes-hall\]](#).
- [42] S. A. Parameswaran, R. Roy, and S. L. Sondhi, *Phys. Rev. B* **85**, 241308 (2012), [arXiv:1106.4025 \[cond-mat.str-el\]](#).
- [43] B. A. Bernevig and N. Regnault, *Phys. Rev. B* **85**, 075128 (2012), [arXiv:1110.4488 \[cond-mat.str-el\]](#).
- [44] A. Boumali and H. Hassanabadi, *EPJ Plus* **128**, 124 (2013).
- [45] C. Barcelo, S. Liberati, and M. Visser, *Living Rev. Rel.* **8**, 12 (2005), [ *Living Rev. Rel.*14,3 (2011) ], [arXiv:gr-qc/0505065v3 \[gr-qc\]](#).
- [46] S. Weinfurter, E. W. Tedford, M. C. J. Penrice, W. G. Unruh, and G. A. Lawrence, *Phys. Rev. Lett.* **106**, 021302 (2011), [arXiv:1008.1911 \[gr-qc\]](#).
- [47] F. Belgiorno, S. L. Cacciatori, M. Clerici, V. Gorini, G. Ortenzi, L. Rizzi, E. Rubino, V. G. Sala, and D. Faccio, *Phys. Rev. Lett.* **105**, 203901 (2010), [arXiv:1009.4634 \[gr-qc\]](#).
- [48] J. Steinhauer, *Nature Phys.* **10**, 864 (2014), [arXiv:1409.6550 \[cond-mat.quant-gas\]](#).
- [49] J. Steinhauer, *Nature Phys.* **12**, 959 (2016), [arXiv:1510.00621 \[gr-qc\]](#).
- [50] F. W. J. Olver, D. W. Lozier, R. F. Boisvert, and C. W. Clark, eds., *NIST Handbook of Mathematical Functions* (Cambridge University Press, New York, NY, 2010) print companion to [28].